This is the peer reviewed version of the following article:

Jugović, Dragana, Miodrag Mitrić, Nikola Cvjetićanin, Boštjan Jančar, Slavko Mentus, and Dragan Uskoković. "Synthesis and Characterization of LiFePO4/C Composite Obtained by Sonochemical Method." *Solid State Ionics* 179, no. 11–12 (May 31, 2008): 415–19. http://dx.doi.org/10.1016/j.ssi.2008.03.014.

Synthesis and characterization of LiFePO$_4$/C composite obtained by sonochemical method

Dragana Jugović, Miodrag Mitrić [*], Nikola Cvjetićanin [**], Boštjan Jančar [***], Slavko Mentus[**], Dragan Uskoković

*Institute of Technical Sciences of the Serbian Academy of Sciences and Arts, Belgrade, Serbia*

[*]*The Vinča Institute of Nuclear Sciences, Belgrade, Serbia*

[**]*Faculty of Physical Chemistry,University of Belgrade, Serbia*

[***] *Jožef Stefan Institute, Ljubljana, Slovenia*

Abstract

Lithium iron phosphate has become of great interest as storage cathode for the next generation of rechargeable lithium batteries. Olivine structure LiFePO$_4$/C composite powder was prepared by ultrasound assisted synthesis. A polyvinyl alcohol solution was used as the source of an in situ formed carbon. X-ray powder diffraction confirmed the phase purity. X-ray powder diffraction data were used for the crystal structure refinement, based on Rietveld full profile method. All relevant structural and microstructural crystal parameters that could be significant for electrochemical intercalation/deintercalation processes were determined. The Rietveld refinement also showed additional electron density on the lithium sites, indicating 3 at.% iron on the lithium site. Electrochemical characteristic of the composite was evaluated by using galvanostatic charge/discharge tests. While cycling at C/3 (C/10) rate the discharge capacity increases, starting from the value of  94.1 (116.0) mAh/g and reaching  99.5 (124.0) mAh/g at the end of the cycling. Particle morphology was revealed by both scanning and transmission electron microscopies. On the thin particle edges carbon film with a typical thickness of several nanometers can be observed, as well as small carbon agglomerates (typical size <6 nm) at certain spots on the substrate surface.

Corresponding author:

Dragana Jugović

Institute of Technical Sciences of the Serbian Academy of Sciences and Arts,

Knez Mihailova 35/IV, 11 000 Belgrade, Serbia,

Phone: +381641177549, Fax: +381112185263, e-mail: djugovic@vinca.rs

# 1. Introduction

Almost all of the research and commercialization of cathode materials for lithium ion batteries has centered on two classes of materials. The first contains layered compounds with an anion close-packed lattice exemplified by first $LiTiS_2$, followed by $LiCoO_2$, $LiNi_{1-y}Co_yO_2$. The spinels, such as $LiMn_2O_4$, may be considered as a special case where transition metal cations are ordered in all the layers. The materials in the second group have more open structures, like many of the vanadium oxides, the tunnel compounds of manganese dioxide, and most recently the transition-metal phosphates, such as the olivine $LiFePO_4$ [1]. The overwhelming advantage of iron-based compounds is that, in addition to being inexpensive and naturally abundant, they are less toxic than Co, Ni, and Mn. $LiFePO_4$ initially includes one $Li^+$ ion per formula unit that can be extracted and transferred to the anode in the first charge process, compensating for the oxidation of iron ($Fe^{2+}$ to $Fe^{3+}$). The theoretical capacity based on this one-electron reaction is 170 mAh/g. At this time, the main obstacle for reaching the theoretical performances of $LiFePO_4$ at ambient temperature is its very low electronic conductivity. Several possible means to overcome this major problem were recently explored: the synthesis of a $LiFePO_4$/electronic conductor composite compound [2, 3, 4], selective doping with supervalent cations to increase the intrinsic electronic conductivity [5, 6, 7], and the achievement of a small and homogeneous particle size distribution [8].

The olivine structure that typifies $LiFePO_4$ has a hexagonally-close-packed oxygen array, in which the octahedra share both edges and faces. The cation arrangement in $LiFePO_4$ differs significantly from that in the layered and spinel structures. There is no continuous network of $FeO_6$ edge shared octahedra that might contribute to electronic conductivity; instead, the divalent $Fe^{2+}$ ions occupy corner-shared octahedra. The phosphorus ions are located in tetrahedral sites, and the lithium ions reside in chains of edge-shared octahedra. Lithium motion in the olivine crystal structure occurs through one-dimensional (1D) channels along the b axis [9].

There are many synthesis routes in preparing $LiFePO_4$: solid-state reaction [2, 10], mechanochemical activation [11, 12, 10], carbothermal reduction method [13], hydrothermal synthesis [14, 11, 15], microwave heating [16], emulsion-drying method [17, 18], etc. Regardless of the great number of the synthesis routes it is not easy to prepare single phased samples. Concerning an iron oxidation state (+2) all of these procedures

require inert or reductive atmosphere to prevent the formation of impurities such as $Li_3PO_4$, $FePO_4$ or other Fe(III) species [10]. The physico-chemical properties of bulk materials are very dependant on the way of synthesis and synthesis conditions. Most of these procedures are both energy and time consuming, and often complex. However, to our knowledge there is no literature data of synthesis of olivine $LiFePO_4$ through sonochemical reaction. Sonochemistry arises from the acoustic cavitation phenomenon, that is, the formation, growth, and implosive collapse of bubbles in a liquid medium [19]. Sonochemical processing has proven to be a useful technique for generating novel materials with unusual properties. Here we present structural, microstructural and electrochemical properties of a composite powder made of olivine-type lithium iron phosphate and carbon, synthesized for the first time by using sonochemical reaction.

## 2. Experimental

The sonochemical reaction was carried out in a reaction vessel which was provided with two side openings for passing gas through the reaction mixture. The reaction mixture, consisting of 30 ml of 1wt% polyvinyl alcohol (PVA) aqueous solution, 25 ml of 0.2 M aqueous solution of $FeSO_4*7H_2O$, and appropriate amount of solid $Li_3PO_4$, was exposed to the ultrasound irradiation. The above mixture was sonicated for one hour by a Vibracell sonicator VCX 750 (Sonics & Materials Inc.) operating at 20 kHz, while reductive gas (75% Ar and 25% $H_2$) was bubbled through it. The reaction product was centrifuged, washed with isopropanol, dried at 120 ℃ under vacuum, and calcined at 600 ℃ in a slightly reductive atmosphere (95% Ar and 5 % $H_2$) for 1.5 hours. Literature data imply that the use of annealing temperature in the range of 500-800℃, depending on precursors, ensures well crystallized samples. This moderate temperature was chosen in order to ensure adequate crystallinity in the compound and to avoid sintering, which increases particle size. A slightly reductive atmosphere was used to prevent the formation of $Fe^{3+}$ species. A special care must be taken when choosing hydrogen content, since more reductive atmosphere can reduce phosphates into phosphides [20]. A PVA solution was used as a source of carbon which would enhance the electronic conductivity and suppress particle growth.

X-ray diffraction data were collected on a Philips PW 1050 diffractometer with Cu-K$\alpha_{1,2}$ radiation (Ni filter) at the room temperature. Measurements were done in $2\theta$ range of 10-120° with scanning step width of 0.02° and 12 s times per step. Crystal structure refinement was based on the Rietveld full profile method [21] using the Koalariet computing program [22].

Electrochemical measurements were carried out in a closed, argon filled two-electrode cell, with metallic lithium as a counter electrode. 1M solution of $LiClO_4$ (p.a., Chemmetall GmbH) in PC (p.a., Honeywell) was used as electrolyte. Working electrodes were made from synthesized material, carbon black and PVDF mixed in 75:20:5 weight percent ratio and deposited on platinum foils from slurry prepared in N-methyl-2-pyrrolidone. Galvanostatic charge/discharge tests were performed between 4.1 and 2.7 V at different current rates.

Thermal analysis of the sample was performed on SDT 2960 simultaneous DSC-TGA TA Instruments in order to determine carbon content [15].

Scanning electron microscopy was performed on JEOL  JSM-6460 LV.

More detailed analysis of particle microstructure was accomplished using transmission electron microscopy, TEM (JEOL  JEM 2000 FX) with acceleration voltage of 200 keV.

For electrical conductivity measurements, pellet was prepared by die-pressing powder with a pressure of 3 tonnes $cm^{-2}$, and then coating with Ag paste on both sides. The disc-shaped pellet was around 0.8 cm in diameter and 0.17 cm in thickness. Conductivity was measured by a Wayne Kerr Universal Bridge B 224 at 1 kHz, in the temperature range from room temperature to 363K.

3. Results and discussion

Powder obtained after ultrasound irradiation and before calcination was completely amorphous as checked by X-ray diffraction measurement. After thermal treatment at 600 ℃ a proper crystallinity was achieved. X-ray powder diffraction pattern was used for the structural analysis of the synthesized sample. The refinement results show that sonochemical reaction gave sample that is well crystallized as single-phase phospho-olivine, without any impurities at detectable level. There is no evidence for the formation of

crystalline carbon, so internal carbon could be treated as a contribution to the background. The amount of an in situ formed carbon was determined by heating the powder in air, and the estimated value was 5wt%. The structure of the LiFePO$_4$ powder has been refined in the space group $P$nma (D$_{2h}^{16}$) in olivine type with following crystallographic positions: Li$^+$ ions in special crystallographic position $4a$ [0,0,0] with local symmetry $\bar{1}$; Fe$^{2+}$ and P$^{5+}$ ions occupy two different crystallographic $4c$ positions [x,0.25,z] with local symmetry m; O$^{2-}$ ions occupy three different crystallographic positions: additional two $4c$ positions and one general $8d$ position [x,y,z] with local symmetry 1. Crystal structure refinement was based on the Rietveld full profile method [21] using the Koalariet computing program based on a Fundamental Parameters convolution approach to generate line profiles. This program is appropriate for processing the data obtained from the samples with dominant microstructure parameters (small crystallite size and large microstrains) [22]. The observed and calculated X-ray diffraction profiles are given in Figure 1, while the main results of the final Rietveld refinement are presented in Table 1. The cell parameters obtained from Rietveld refinement are a = 10.3149(6) Å, b = 5.9984(4) Å, c = 4.7010(3) Å, and volume V = 290.86(3) Å$^3$, consistent with literature data obtained for the powder synthesized by solid state reaction [23]. The Rietveld refinement also showed additional electron density on the lithium sites, indicating 3 at.% iron on the lithium site. Microstructural parameters data showed that sonochemical method is convenient for obtaining small particles of LiFePO$_4$, which are suitable for ensuring a good connection with a conductive carbon. Both refined and fixed fractional atomic coordinates were used for the calculation of all relevant bond distances and bond angles that enabled us to determine coordination polyhedra. Some relevant bond distances are provided in Table 2. The calculated average Fe-O bond distance is smaller while the average P-O distance is larger than those obtained for the powder synthesized by solid state reaction [23], implying weaken P-O bonding and strengthen Fe-O bonding. This could be explained through an Fe-O-P inductive effect. The inductive effect may be described as the action of one group to affect electrostatically the electron distribution in other group. Thus, a change in distribution of the electrons modifies the force constant of the chemical bonds.

The measured a.c. conductivity data were arranged in a standard Arrhenius plot $\sigma = \sigma_0 exp(-E_a/k_BT)$ (Figure 2), where $E_a$ is the activation energy. These results show a usual increase of the conductivity with increasing temperature. The observed room temperature value was within the order of magnitude of 10$^{-6}$

5

Scm$^{-1}$, which is notably higher than $10^{-8}$ S cm$^{-1}$ characteristic of the carbon-free LiFePO$_4$ sample [3]. Furthermore, plot of log($\sigma$) vs. 1/T was found to be linear in the temperature range considered.

Figure 3 shows particle morphology of the sample revealed by scanning electron microscopy. The particles are irregular in shape and agglomerated, with mean size 200-300 nm. By comparing these results with the mean crystallite size of 70 nm obtained from XRPD analysis (Table 1) it can be concluded that polycrystalline particles are composed of large number of crystallites. In addition, energy dispersive spectroscopy (EDS) of the sample showed only peaks corresponding to Fe, P, C, and O. Li is too light for the detection with EDS. More detailed analysis of particle microstructure was accomplished using TEM images (Figure 4). The electron diffraction, taken from a part of Figure 4a shows the presence of LiFePO$_4$ phase with the domains mainly oriented along [001] axis (inset of Fig. 4a). Due to pronounced particle agglomeration, grain boundaries are not quite clear, and within a relatively broad grain size distribution, average grain size was estimated to be about 30 – 40 nm. On the thin particle edges (Figure 4b) carbon film with a typical thickness of several nanometers can be observed. We believe that this carbon layer is responsible for improved electrical conductivity. Apart from that, high carbon content leads to the formation of small carbon agglomerates (typical size <6 nm) at certain spots on the substrate surface (Figure 4c). Similar findings have already been reported in the literature [24, and references therein] for carbon coated composites synthesized by citrate gel combustion.

Electrochemical performance of the sample used as a cathode of a Li-ion battery, was examined by charge-discharge tests. The cyclings were done between 2.7 and 4.1 V and the current densities were 59.7 and 17.8 mA/g, which correspond nearly to C/3 and C/10 rate, respectively. Figure 5 shows discharge curves at C/3 rate. A flat plateau at around 3.4 V is observed during both charge and discharge. Resulted specific capacities were calculated based on the mass of pure LiFePO$_4$. It is interesting to notice that discharge capacity increases during cycling, starting from the value of 94.1 mAh/g for the first cycle and reaching 99.5 mAh/g at the end of the fiftieth cycle (inset of Fig.5). This behavior is markedly different from the conventional olivine LiFePO$_4$ whose capacity increases slightly in the initial several cycles and then remains stable [8] or decreases [18]. Similiar behavior was also observed when smaller current rate of 17.8 mA/g was used, (Fig. 6). Then, the capacity increased from 116 mAh/g in the first discharge to 124 mAh/g in the fifteenth discharge. During structural refinement, it was shown that part of lithium sites (3%) are occupied by

6

iron ions. Iron ion positioned on lithium site could block the whole channel and prevents lithium motion, leaving isles of $LiFePO_4$ domains in the $FePO_4$ surround, and causing smaller specific capacity as a result. Capacity increase observed during cycling suggests structural relaxation most likely through ordering of the iron ions. This may be the explanation for the decrease in microstrain observed in cycled material.

4. Conclusion

We have shown that olivine structured $LiFePO_4$/C composite can be successfully synthesized combining sonochemical precipitation and calcination. The main advantage of this method is the formation of an in situ C-coated $LiFePO_4$ nanostructured powder of high purity, which provides homogeneous material with improved electrical conductivity. This method may also be suitable for selective doping with supervalent cations to increase the intrinsic electronic conductivity of $LiFePO_4$ powder.

References

[1]     M. S. Whittingham, Lithium Batteries and Cathode Materials, Chem. Rev. 104 (2004) 4271.

[2]     Marca M. Doeff, Yaoqin Hu, Frank McLarnon, and Robert Kostecki, Electrochem. Solid-State Lett., 6 (2003) A207.

[3]     S.-T. Myung, Sh. Komaba, N. Hirosaki, H. Yashiro, N. Kumagai, Electrochim. Acta, 49 (2004) 4213.

[4]     Z. Chen and J. R. Dahn, J. Electrochem. Soc., 149 (2002) A1184.

[5]     S.-Y. Chung, J.T. Bloking, and Y.-M. Chiang, Nature Mater., 1 (2002) 123.

[6]     G. X. Wang, S. Needham, J. Yao, J.Z. Wang, R. S. Liu, H. K. Liu, J. Power Sour. 159 (2006) 282.

[7]     C. Delacourt, C. Wurm, L. Laffont, J.-B. Leriche, C. Masquelier, Solid State Ionics 177 (2006) 333.

[8]     A. Yamada, S. C. Chung, and K. Hinokuma, J. Electrochem. Soc., 148 (2001) A224.

[9]     D. Morgan, A. Van der Ven, G. Ceder, Electrochem. Solid-State Lett. 7 (2004) A30.

[10]    S. Franger, F. Le Cras, C. Bourbon, and H. Rouault, J. Power Sour., 119-121 (2003) 252.

[11]    S. Franger, F. Le Cras, C. Bourbon, and H. Rouault, Electrochem. Solid-State Lett., 5 (2002) A231.

[12]    N. Kosova, E. Devyatkina, Solid State Ionics, 172 (2004) 181.

[13]    J. Barker, M. Y. Saidi, and J. L. Swoyer, Electrochem. Solid-State Lett., 6 (2003) A53.

[14]    Sh. Yang, P. Y. Zavalij, M. S. Whittingham, Electrochem. Commun., 3 (2001) 505.

[15]    Sh. Yang, Y. Song, P. Y. Zavalij, M. S. Whittingham, Electrochem. Commun. 4 (2002) 239.

[16]    K.S.Park, J.T.Son, H.T.Chung, S.J.Kim, C.H.Lee, and H.G.Kim, Electrochem. Commun., 5 (2003) 839.

[17]    T.-H. Cho, H.-T. Chung, J. Power Sour., 133 (2004) 272.

[18]    S.-T. Myung, Sh. Komaba, N. Hirosaki, H. Yashiro, N. Kumagai, Electrochim. Acta, 49 (2004) 4213.

[19]    K. S. Suslick, G. J. Price, Annu. Rev. Mater. Sci., 29 (1999) 295.

[20]    G. Arnold, J. Garche, R. Hemmer, S. Ströbele, C. Vogler, M. Wohlfahrt-Mehrens, J. Power Sour. 119-121 (2003) 247.

[21]    H.M. Rietveld: J. Appl. Cryst. 2 (1969) 65.

[22]    R.W. Cheary, A. Coelho: J. Appl. Cryst., **25** (1992) 109.

[23]    A. S. Andersson, B. Kalska, L. Häggström, J. O. Thomas, Solid State Ionics, 130 (2000) 41.

[24]    J. Moskon, R. Dominko, R. Cerc-Korosec, M. Gaberscek and J. Jamnik, J. Power Sour., (2007), doi:10.1016/j.jpowsour.2007.06.239.

Table captions

Table 1. The final results of the structural refinement for LiFePO$_4$ sample.

Table 2. Selected bond lengths (in Å) for LiFePO$_4$.

| Lattice parameters [Å] | a = 10.3149(6) | | | |
| --- | --- | --- | --- | --- |
| | b = 5.9984(4) | | | |
| | c = 4.7010(3) | | | |
| Primitive cell volume [Å$^3$] | V = 290.86(3) | | | |
| Mean crystallite size [nm] | 70(10) | | | |
| Microstrain [%] | 0.23(2) | | | |
| fractional coordinates | x | y | z | Fe occ. |
| Li    (4$a$) | 0 | 0 | 0 | 0.03 |
| Fe   (4$c$) | 0.2810(1) | 0.25 | 0.9710(3) | 0.97 |
| P    (4$c$) | 0.09475(2) | 0.25 | 0.4191(4) | 0 |
| O(1) (4c) | 0.09845(4) | 0.25 | 0.7336(7) | 0 |
| O(2) (4c) | 0.4431(5) | 0.25 | 0.2146(5) | 0 |
| O(3) (8d) | 0.1641(3) | 0.0440(4) | 0.2761(4) | 0 |
| | B  [Å$^2$] | | | |
| Li | 1.3(2) | | | |
| Fe | 0.17(4) | | | |
| P | 0.38(5) | | | |
| O1 | 0.8(1) | | | |
| O2 | 0.4(1) | | | |
| O3 | 0.7(1) | | | |
| R factors [%] | $R_{wp}$  2.3 <br> $R_B$  3.6 | | | |

Table 1

| M-O bond | Length [Å] |
|---|---|
| Fe – O(1) | 2.1888 |
| Fe – O(2) | 2.0264 |
| Fe – O(3) x 2 | 2.2449 |
| Fe – O(3)' x 2 | 2.0664 |
| (Fe – O)$_{ave}$ | 2.1396 |
| Li – O(1) x 2 | 2.2018 |
| Li – O(2) x 2 | 2.0962 |
| Li – O(3) x 2 | 2.1491 |
| (Li – O)$_{ave}$ | 2.1490 |
| P – O(1) | 1.4791 |
| P – O(2) | 1.6859 |
| P – O(3) x 2 | 1.5780 |
| (P – O)$_{ave}$ Table 2 | 1.5802 |
| O(1) – O(2) | 3.0310 |
| Li – Li | 2.9992 |

Table 2

Figure captions

Fig. 1. The observed (•), calculated (-), and difference (bottom) X-ray diffraction data of LiFePO$_4$ taken at room temperature. Vertical markers bellow the diffraction patterns indicate positions of possible Bragg reflections.

Fig. 2 Arrhenius plot of electrical conductivity for synthesized sample.

Fig. 3 SEM micrograph of composite LiFePO$_4$/C powder.

Fig. 4 TEM images of LiFePO$_4$/C composite: a) electron diffraction pattern with the domains mainly oriented along [001] axis; b) arrows point out 2-3 nm thick layer of amorphous carbon; c) small carbon agglomerates can be seen as spots on the substrate surface.

Fig. 5  Cycle performance for LiFePO$_4$/C at C/3 rate. The inset shows capacity vs. cycle number.
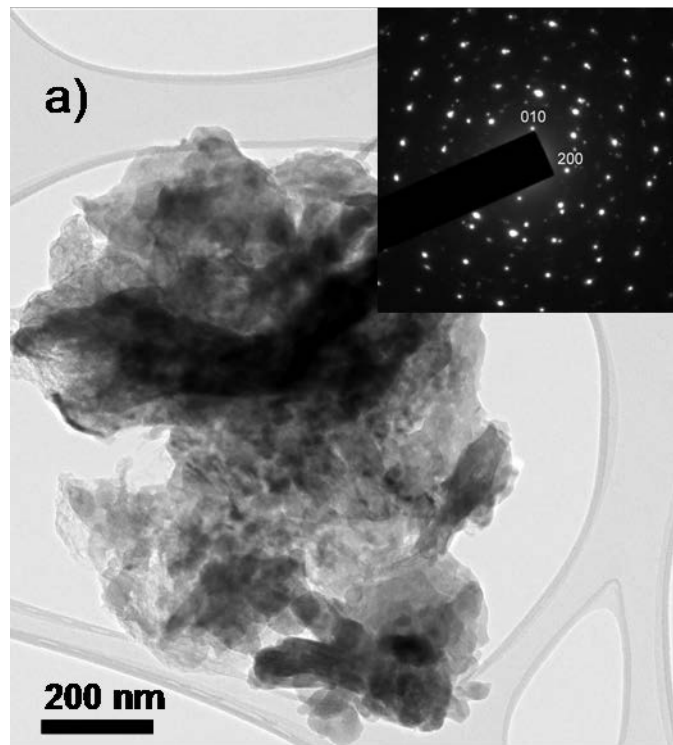
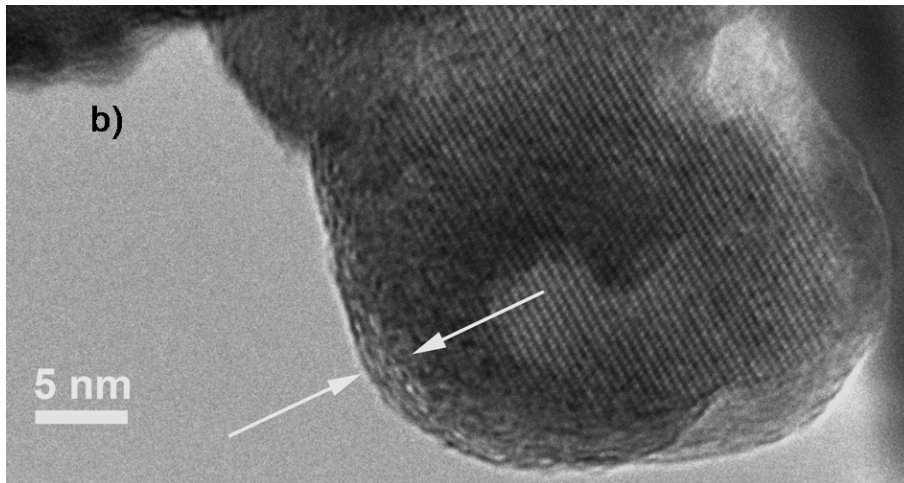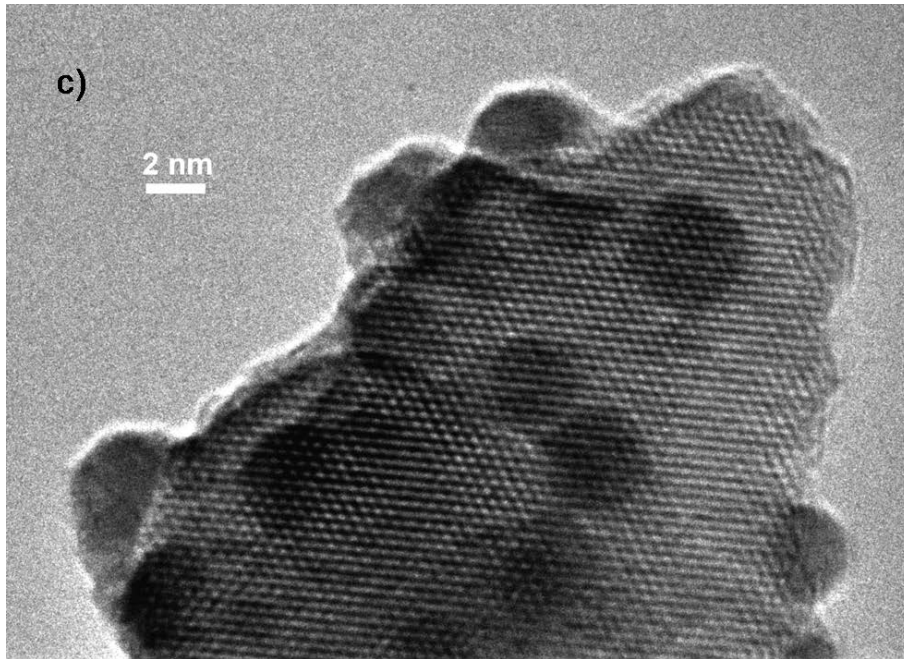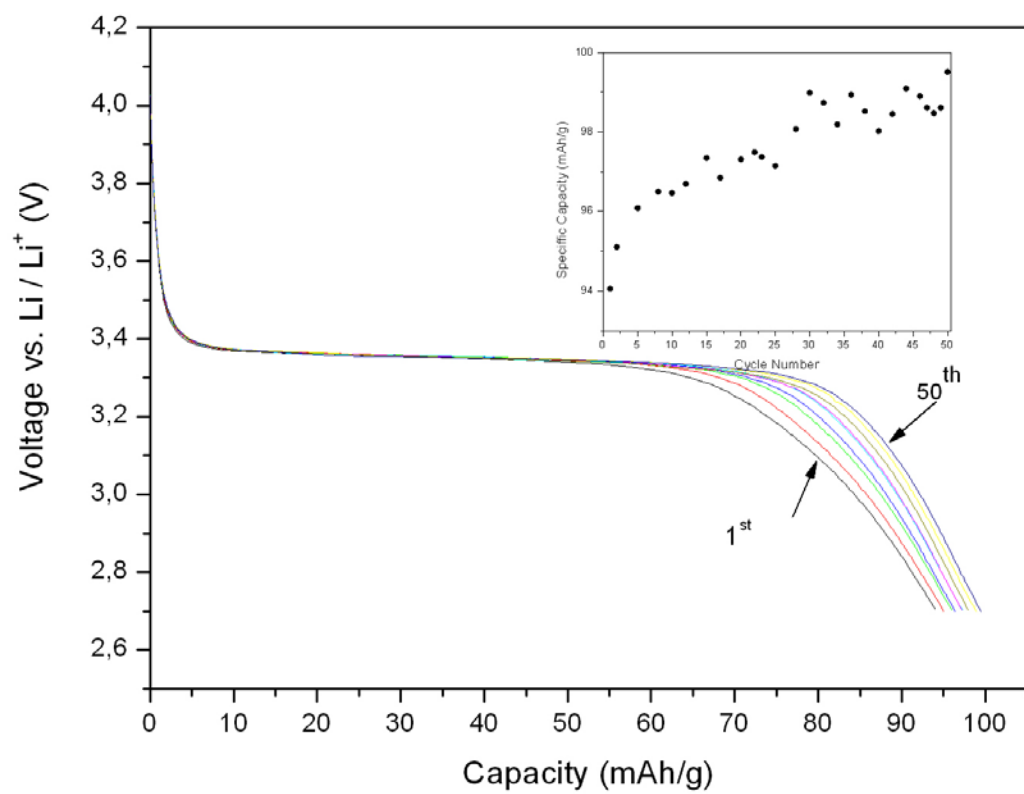Fig. 6 Cycle performance for LiFePO$_4$/C at C/10  rate.
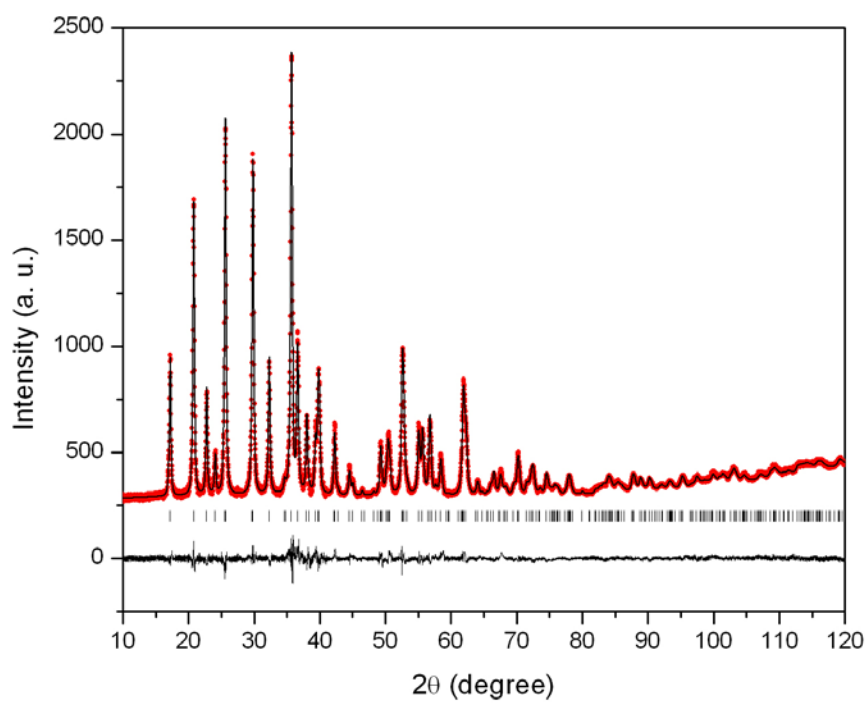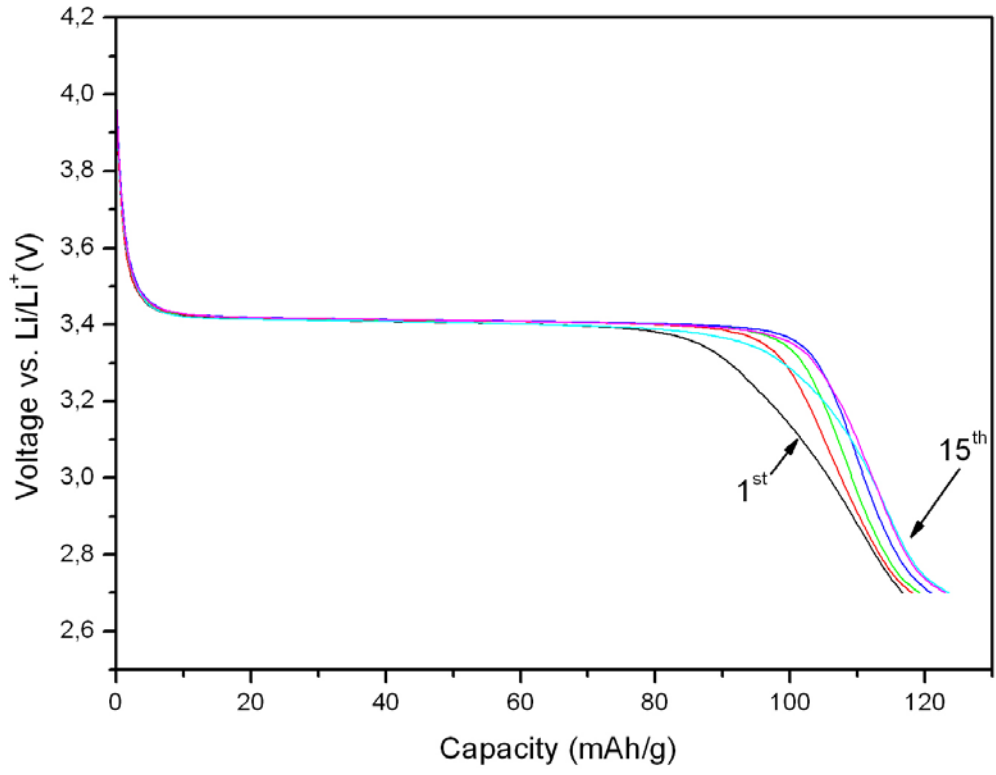
Figure 1
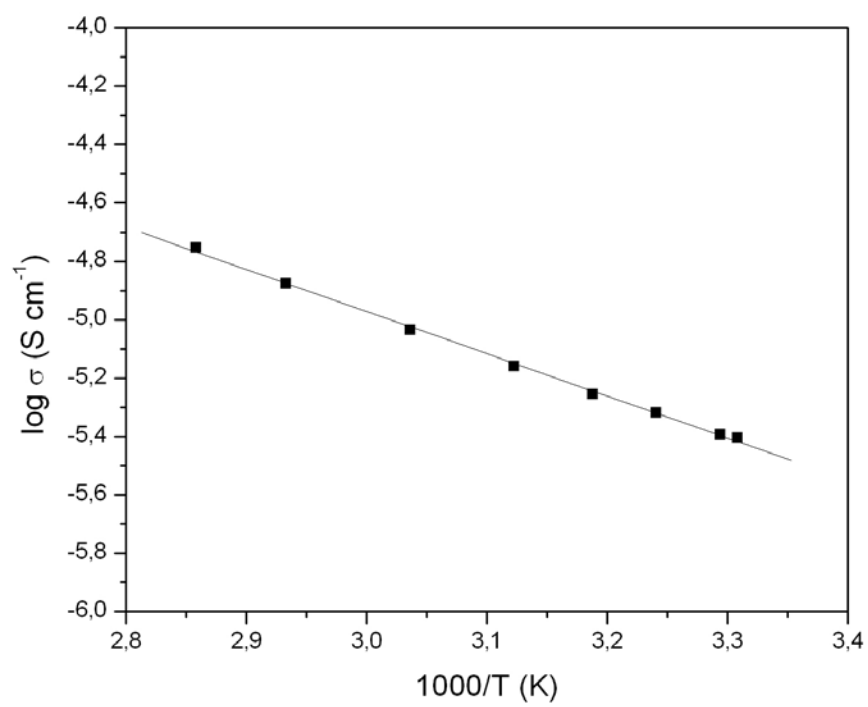
Figure 2
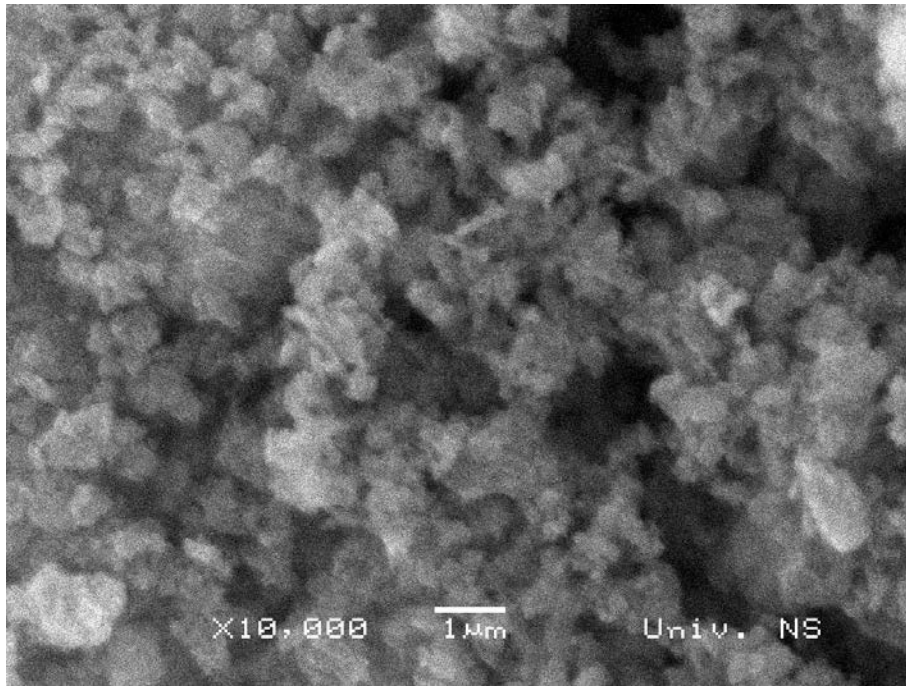
Figure 3

Figure 4a

Figure 4b

Figure 4c

Figure 5

Figure 6